Non-Metric Calibration of Wide Angle Lenses *

Rahul Swaminathan and Shree K. Nayar
Department of Computer Science
Columbia University
New York, NY 10027

Abstract

Images taken with wide-angle cameras tend to have severe distortions which pull points towards the optical center. This paper proposes a new method for recovering the distortion parameters without using any calibration objects. The distortions cause straight lines in the scene to appear as curves in the image. Our algorithm seeks to find the distortion parameters that would map the image curves to straight lines. The user selects a small set of points along the image curves. Recovery of the parameters is formulated as the minimization of an objective function which is designed to explicitly account for noise in the selected image points. Experimental results are provided for synthetic data with different noise levels as well as for real images. The computed distortion parameters are used to undistort a video stream in real time, using a look-up table.

1 Introduction

It is desirable in most surveillance applications to capture the region of interest with as few cameras as possible. Wide-angle cameras help in this regard, but at the cost of severe image distortions. Wide-angle lenses that adhere to perspective projection would necessitate the use of prohibitively large image detectors. These lenses are therefore designed to severely bend rays of light around the periphery of the field of view[1], thus permitting the use of a small image detector (say, a CCD). The effects of the resulting image distortions are clearly visible in Figure 1.

Images from surveillance cameras are used essentially for monitoring by humans, or for further visual processing. In either case, it is desirable that wide-angle distortions be removed. If the optics of the wide-angle camera system are known *apriori* (i.e. the distortion parameters), then distortion correction can be easily applied using the known parameters. Unfortunately, such information is seldom revealed by manufacturers. Furthermore, in mass production, optical characteristics are sure to vary from one lens to the next. It is therefore desirable to have a simple calibration method for extracting the distortion parameters of each lens. This paper presents such a calibration method.

Figure 1: Images captured with wide-angle cameras have severe distortions that can alter the appearances of objects in the scene.

Many calibration methods have been suggested for recovering lens distortion parameters. Tsai [1987] used known points in 3D space to recover some of the distortion parameters. Goshtasby [1989] utilized Bezier patches to model the distortions and used a uniform grid placed in front of the camera as a calibration object. Weng [1992] also used calibration objects to extract all the distortion parameters. All these methods fall in the category of "stellar" calibration [Brown, 1971].

In contrast, Brown [1971] proposed a "non-metric" approach that does not rely on known scene points. Instead, he relies on the fact that straight lines in the scene must always perspectively project to straight lines in the image. An iterative least-squares formulation is used to estimate distortion parameters which map distorted image curves to straight lines. Brown's algorithm relies on essentially noiseless image data, which is obtained by imaging plumb-lines suspended against a black background. More recently, Kang [1997] used snakes to

*This work was supported in part by the ONR/DARPA MURI program under ONR Contract No. N00014-95-1-0601. Several other agencies and companies have also supported aspects of this research.

[1]The bending of light rays, typically leads to a non-singular entrance pupil. The resulting locus of pupils in three dimensions is called a *diacaustic* [Born and Wolf, 1965]. This implies that, for a wide-angle lens, complete removal of distortions cannot be achieved. For our purposes, we will assume a small pupil locus that can be approximated by a single point.

represent the distorted curves instead of discrete points. Becker [1995] used three mutually orthogonal sets of parallel lines and a vanishing point constraint to recover distortion parameters. In [Stein, 1997], point correspondences in multiple images are used to estimate radial distortions.

Previous work suffers from one or more of the following restrictions: calibration objects need to be used, not all the distortion parameters are recovered, or the algorithm is highly sensitive to noise. One exception is the work of Becker [1995]. However, Becker's constraint (triplets of orthogonal lines) is less abundant in urban settings than the randomly oriented straight lines we use. In addition, while Becker uses the Normal distribution to model noise, our algorithm makes no assumptions about the exact nature of noise in the selected image points. We formulate the estimation of distortion parameters as the minimization of a noise insensitive objective function via efficient search. Experimental results with synthetic and real data are presented, which demonstrate the robustness of the proposed method, in the presence of large amounts of noise.

2 Distortion Model

Let the true perspective projection of a scene point be $\mathbf{q}'$ (see Figure 2). Due to distortions in the lens, the point gets transformed to a new point $\mathbf{q}$. Let (x, y) be the Cartesian and (r, ϕ) be the polar coordinates of $\mathbf{q}$, similarly let (x', y') be the Cartesian and (r', ϕ') be the polar coordinates of $\mathbf{q}'$. Also let the optical center C be located at (x_p, y_p). Then, the Cartesian and polar coordinates are related as:

$$r = \sqrt{\bar{x}^2 + \bar{y}^2} \ , \ \tan(\phi) = \frac{\bar{y}}{\bar{x}}$$

where

$$\bar{x} = x - x_p \ , \ \bar{y} = y - y_p \, . \tag{1}$$

The distortion of $\mathbf{q}'$ can be split into three components: (1) shift of the image center, (2) radial distortion, and (3) decentering distortion. The first of these is given by (x_p, y_p), while the remaining two we will now describe in greater detail.

2.1 Radial Distortions

Radial distortions in most wide-angle cameras pull points towards the optical center. This kind of distortion is also referred to as *barrel distortion* [Born and Wolf, 1965]. This effect is radially symmetric and depends solely on the distance from the optical center. The radial distortion present in the point $\mathbf{q}$ is:

$$\Delta r(\mathbf{q}) = \sum_{i=1}^{\infty} C_{2i+1} r^{2i+1} \, , \tag{2}$$

where, C_{2i+1} are the distortion parameters. Terms higher than the fifth-order one can be ignored as their contribution to the distortion is negligible in practice [Brown, 1966]. Hence, we have:

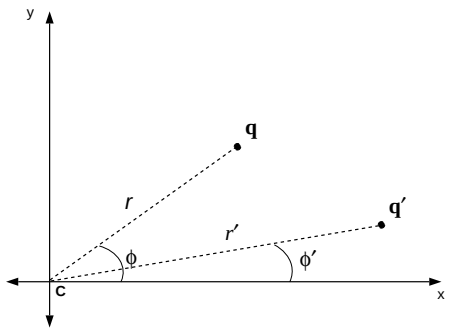

Figure 2: $\mathbf{q}'$ is the perspective projection of a scene point onto the image plane. Due to radial and decentering distortions, $\mathbf{q}'$ gets mapped to the point $\mathbf{q}$.

$$\Delta r(\mathbf{q}) \quad \approx \quad C_3 r^3 + C_5 r^5 \ . \tag{3}$$

2.2 Decentering Distortions

Decentering distortions are caused by the non-orthogonality of the lens components with respect to the optical axis. It is highly unlikely for an imaging system to have no decentering distortions, which, unlike radial distortions, act tangentially. We use Conrady's model[Conrady, 1919] for decentering distortion:

$$\begin{aligned} \Delta T_x(\mathbf{q}) &= [P_1 r^2 (1 + 2\cos^2(\phi)) + 2P_2 r^2 \sin(\phi)\cos(\phi)] \\ &\quad [1 + \sum_{i=1}^{\infty} P_{i+2} r^{2i}] \\ \Delta T_y(\mathbf{q}) &= [P_2 r^2 (1 + 2\sin^2(\phi)) + 2P_1 r^2 \sin(\phi)\cos(\phi)] \\ &\quad [1 + \sum_{i=1}^{\infty} P_{i+2} r^{2i}] \, , \end{aligned} \tag{4}$$

where, $P_1, P_2, \ldots$ are the distortion parameters and $\Delta T_x, \Delta T_y$ are the distortions along the x and y directions, respectively.

The higher-order terms in the above expression are relatively insignificant. Hence, P_1 and P_2 are generally sufficient for modeling decentering [Brown, 1966]:

$$\begin{aligned} \Delta T_x(\mathbf{q}) &\approx [P_1 r^2 (1 + 2\cos^2(\phi)) + 2P_2 r^2 \sin(\phi)\cos(\phi)] \\ \Delta T_y(\mathbf{q}) &\approx [P_2 r^2 (1 + 2\sin^2(\phi)) + 2P_1 r^2 \sin(\phi)\cos(\phi)] \, . \end{aligned} \tag{5}$$

2.3 Complete Distortion Model

The total distortion is obtained as a sum of the above components:

$$\begin{aligned} \Delta x(\mathbf{q}) &\approx \cos(\phi)[\Delta r(\mathbf{q})] + \Delta T_x(\mathbf{q}) \\ \Delta y(\mathbf{q}) &\approx \sin(\phi)[\Delta r(\mathbf{q})] + \Delta T_y(\mathbf{q}) \end{aligned} \tag{6}$$

In order to correct distortions, we need to recover the parameters $(C_3, C_5, P_1, P_2, x_p, y_p)$.

3 Objective Function Formulation

The constraint used in this paper is that, under perspective projection, straight lines in the scene should project to straight lines in the image. We assume that the user of our calibration method knows which (distorted) image curves correspond to straight lines in the scene. Based on this knowledge, the user selects points along image curves. In this setting, an objective function can be defined, which when minimized, yields the parameters that map the distorted points to lie on straight lines. We present three objective functions, namely, sum of squared distances (from straight lines), normalized sum of squared distances and one that explicitly estimates noise in the chosen image points. The first two are presented mainly to demonstrate that simple objective functions (similar to ones proposed previously) are highly noise sensitive. In contrast, the third function is designed to explicitly account for noise in the image points chosen by the user. All our objective functions are non-linear and are minimized using efficient search algorithms. In what follows our goal will be to recover only the radial and decentering distortion parameters. The shift of optical center (x_p, y_p) will be recovered separately in an iterative fashion.

3.1 Sum of Squared Distances (ξ_1)

This objective function is similar to the one used in the iterative least-squares method developed by Brown [1971]. In our approach, during search, a set of (hypothesized) distortion parameters $\mathcal{S} = \{C_3, C_5, P_1, P_2\}$ are applied to the selected image points $\mathbf{q}(x, y)$. Lines are fitted to the resulting points $\mathbf{q}'(x', y')$ and the objective function is computed as the sum of the squared distances of the points from their corresponding "best-fit" lines.

Let the best-fit line for a set of points $\mathbf{q}'$ (originally, on the same image curve) be:

$$x' \sin(\theta) - y' \cos(\theta) + \rho = 0 \ , \tag{7}$$

where, θ is the angle the line makes with the horizontal axis and ρ is the distance of the line from the image center. Therefore, the error due to a single point is given by:

$$e_1 = (x' \sin(\theta) - y' \cos(\theta) + \rho)^2 \ ,$$

where

$$x' = x + \Delta x(\mathbf{q}) \ , y' = y + \Delta y(\mathbf{q}) \ . \tag{8}$$

Let the number of curves selected by the user be L, and let the number of points on each line l be P_l. Then, the objective function is given by:

$$\xi_1 \quad = \quad \sum_{l=1}^{L} \left[\sum_{p=1}^{P_l} \left(x'_{p,l} \sin(\theta_l) - y'_{p,l} \cos(\theta_l) + \rho_l \right)^2 \right] \ . \tag{9}$$

where θ_l and ρ_l are the best-fit line parameters corresponding to image curve l and $(x_{p,l}, y_{p,l})$ is the p^{th} point on line l.

3.2 Normalized Sum of Squares (ξ_2)

Although simple, the above formulation is very sensitive to noise. From the distortion model, it can be seen that noise is magnified by the higher-order distortion terms in $\mathcal{S}$ (in particular, the third- and fifth-order terms). As a result, points that lie closer to the image center contribute less to the error than points further away. This effect is partially remedied by normalizing the error e_1 by the square of the distance ρ_l of the corresponding line l from the image center. Then, the modified objective function is:

$$\xi_2 \quad = \quad \sum_{l=1}^{L} \left[\sum_{p=1}^{P_l} \left(\frac{x'_{p,l} \sin(\theta_l) - y'_{p,l} \cos(\theta_l) + \rho_l}{\rho_l} \right)^2 \right] \tag{10}$$

3.3 Explicit Noise Estimation (ξ_3)

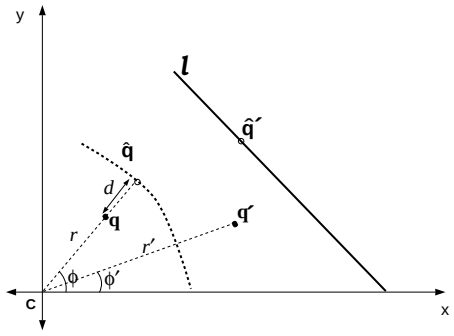

Figure 3: $\mathbf{q}$ is a point selected by the user and $\mathbf{q}'$ is its undistorted location on applying the (hypothesized) distortion parameters $\mathcal{S}$. l is the "best-fit" line estimated for all $\mathbf{q}'$, which are believed to lie on the same scene line. $\hat{\mathbf{q}}$ is a point close to $\mathbf{q}$ such that, its undistorted location $\hat{\mathbf{q}}'$ (obtained by applying $\mathcal{S}$ on $\hat{\mathbf{q}}$) lies on l. d is the distance between $\mathbf{q}$ and $\hat{\mathbf{q}}$, which we wish to minimize.

The previous objective functions, ξ_1 and ξ_2 are defined in the space of the undistorted points (i.e. after applying $\mathcal{S}$). Since noise in the selection process is induced in the distorted coordinates, it is more appropriate to formulate an objective function that uses errors computed in the space of distorted image points, so as to avoid non-linear biases inherent to our distortion model.

As shown in Figure 3, let $\mathbf{q}$ be the distorted point under consideration and $\mathbf{q}'$ be the "undistorted" point obtained by applying the set of distortion parameters $\mathcal{S}$. Again, l is the best-fit line for the points $\mathbf{q}'$. We now determine (via search) the point $\hat{\mathbf{q}}$ close to $\mathbf{q}$, which when undistorted using $\mathcal{S}$ would lie on l at $\hat{\mathbf{q}}'$. The new error function is defined as:

$$e_3 = \|\mathbf{q} - \hat{\mathbf{q}}\|^2 \ . \tag{11}$$

Since $\hat{\mathbf{q}}'(\hat{x}', \hat{y}')$ must lie on l, it must satisfy the constraint:

$$\hat{x}' \sin(\theta) - \hat{y}' \cos(\theta) + \rho = 0 \ ,$$

where: $\hat{x}' = \hat{x} + \Delta x(\hat{\mathbf{q}})$, $\hat{y}' = \hat{y} + \Delta y(\hat{\mathbf{q}})$. (12)

Using all the selected points, the objective function is determined as:

$$\xi_3 = \sum_{l=1}^{L} \left(\sum_{p=1}^{P_l} \|\mathbf{q}_{p,l} - \hat{\mathbf{q}}_{p,l}\|^2 \right) . \quad (13)$$

4 Minimization of ξ_1, ξ_2 and ξ_3

We now describe the non-linear search algorithms used to recover the distortion parameters $\mathcal{S}$ by minimizing the objective functions ξ_1 , ξ_2 and ξ_3. It should be noted that our calibration method is in no way restricted to the specific search algorithms we have used.

We used a modified simplex search algorithm outlined in [Nelder and Mead, 1965], implemented in the IMSL library. This implementation requires upper and lower bounds on the parameters to be estimated. The bounds we have chosen can model distortions more severe than those found in typical wide-angle imaging systems. The following bounds were used: $C_3 : (-10^{-5}, 10^{-5})$, $C_5 : (-10^{-9}, 10^{-9})$, $P_1 : (-10^{-5}, 10^{-5})$, $P_2 :(-10^{-5}, 10^{-5})$.

At each step of the non-linear search, given the set of (hypothesized) parameters $\mathcal{S}$, we must compute the objective function. Computation of ξ_1 and ξ_2 is straightforward, using a linear least-squares method to fit the lines l. However, computing ξ_3 also requires the estimation of the points $\hat{\mathbf{q}}$ (see (12)), for which there is no closed-form solution.

We solve for each $\hat{\mathbf{q}}_{p,l}$ by searching the neighborhood of $\mathbf{q}_{p,l}$ for the point which, when undistorted using $\mathcal{S}$, lies on l. This requires a $2D$ search and is computationally intensive as it needs to be done for every point selected by the user. To speed-up the search for $\hat{\mathbf{q}}$ we formulate the search in a single dimension, since there always exists a point in the radial direction of the selected point, which lies on the true distorted curve. This approximation enables us to estimate the distortion parameters (C_3, C_5, P_1, P_2), in under 1 minute on a 300MHz PC.

4.1 Recovering the Optical Center

Note that we did not include the optical center $C(x_p, y_p)$, in the non-linear search for the distortion parameters $\mathcal{S}$. Initial experiments revealed that including $C(x_p, y_p)$ produced unstable results in the presence of noise. Therefore, we recommend nesting the estimation of (C_3, C_5, P_1, P_2) within a coarse-to-fine search for the optical center.

5 Synthetic Experiments

To evaluate the robustness of our calibration techniques, it is imperative to test them in the presence of noise. Noise enters the system from three main sources: human error in selecting points in the image, CCD quantization and the fact that lines in the scene need not be perfectly straight. It is difficult to quantify the robustness of any calibration method using only real images, due to lack of ground truth. Hence, we synthesize image points needed by the methods discussed earlier.

Points were randomly sampled from synthetically generated lines with random orientations and positions (see Figure 4(a)). Using known distortion parameters, the sampled points were distorted (see Figure 4(b)). To simulate erroneous point selection, we added uniform noise in the interval $(-w, +w)$ (see figure 4(c)). We then used our algorithm to estimate the distortion parameters from the noisy data and used these parameters to undistort the noiseless image points (see Figure 4(d)).

5.1 Measurement of accuracy

Although precise recovery of the distortion parameters $\mathcal{S}$ ensures an exact match between the sampled points (Figure 4 (a)) and the undistorted points (Figure 4 (d)), it is not necessary for accurate distortion correction. A good measure of accuracy and robustness is the distance between the initial position (see Figure 4(a)) and the recovered position (see Figure 4(d)) for each point. We tested each objective function using lines $\mathcal{L}$ of different orientations and positions , various distortion parameters $\mathcal{S}$ and several noise levels in the interval $w = (0, 5)$ pixels.

Tables 1(a), 1(b) and 1(c) show the errors present in the recovered undistorted points using the sum of squares ξ_1, normalized sum of squares ξ_2 and the noise estimation method ξ_3 respectively. Errors are defined as the average of the distances between each of the undistorted points and the original sampled points. Notice the sharp degradation of robustness for large amounts of noise in the simple sum of squares approach (ξ_1) (see Table 1(a)). Although ξ_2 seems better than ξ_1 for certain noise levels, its does not maintain that degree of robustness for high levels of noise. In contrast ξ_3, is much more robust as can be seen from Table 1(c), even at high noise levels.

Table 2 contains more exhaustive results of objective function ξ_3 for different line orientations and distortions parameters. All these experiments clearly demonstrate the robustness of ξ_3 over the others. In most of the cases ξ_3 seems to have sub-pixel accuracy in undistorting the image points even with high levels of noise.

As mentioned earlier, recovery of the shift parameters is implemented as a coarse-to-fine search near the image center. The search for the optical center was done using a 5x5 grid and grid resolutions of 10, 5 and 2 pixels. As Table 3 indicates, fine searches in the presence of noise can result in inaccurate solutions, while coarse searches appear to give better results. The time taken to recover all six distortion parameters $(C_3, C_5, P_1, P_2, x_p, y_p)$ is linear in the number of grid points being searched. Our experiment with a 5x5 grid took about 20 minutes.

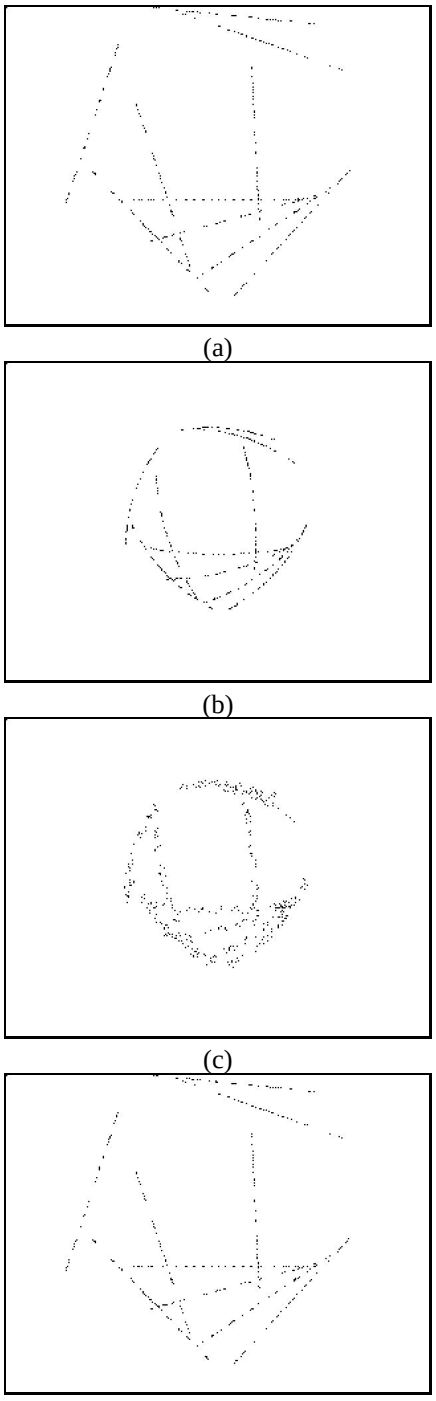

Figure 4: (a) Points randomly sampled from synthetically generated lines. (b) Known distortions are applied to the points in (a). (c) Uniformly distributed random noise in the interval (-5, 5) is added to the distorted points in (b). (d) The distortion parameters are recovered using the algorithm based on objective function ξ_3 and these noisy image points as data. These parameters are used to undo the distortions present in (b). Despite the large amount of noise, recovery of undistorted image points is robust.

Table 1(a): Experimental results for ξ_1.

Distortion Coefficients					Average Error (pixels)			
$\mathcal{L}$	C_3	C_4	P_1	P_2	$w=0$	$w=1$	$w=2$	$n=5$
#1	10^{-5}	10^{-9}	10^{-5}	10^{-5}	0.000	3.360	13.973	42.521
	10^{-5}	10^{-9}	0.000	0.000	0.000	3.264	13.917	42.574
#2	10^{-5}	10^{-9}	10^{-5}	10^{-5}	0.000	12.095	39.567	66.817
	10^{-5}	10^{-9}	0.000	0.000	0.000	12.184	39.616	66.849

Table 1(b): Experimental results for ξ_2.

Distortion Coefficients					Average Error (pixels)			
$\mathcal{L}$	C_3	C_5	P_1	P_2	$w=0$	$w=1$	$w=2$	$n=5$
#1	10^{-5}	10^{-9}	10^{-5}	10^{-5}	0.000	0.356	2.473	12.383
	10^{-5}	10^{-9}	0.000	0.000	0.000	0.396	2.272	12.373
#2	10^{-5}	10^{-9}	10^{-5}	10^{-5}	0.000	1.618	5.448	28.639
	10^{-5}	10^{-9}	0.000	0.000	0.000	1.592	5.550	28.711

Table 1(c): Experimental results for ξ_3.

Distortion Coefficients					Average Error (pixels)			
$\mathcal{L}$	C_3	C_5	P_1	P_2	$w=0$	$w=1$	$w=2$	$n=5$
#1	10^{-5}	10^{-9}	10^{-5}	10^{-5}	0.002	0.363	0.390	0.398
	10^{-5}	10^{-9}	0.000	0.00	0.003	0.328	0.273	0.318
#2	10^{-5}	10^{-9}	10^{-5}	10^{-5}	0.008	0.663	0.773	0.502
	10^{-5}	10^{-9}	0.000	0.000	0.006	0.529	0.734	0.330

Table 2: Detailed experimental results for ξ_3.

Distortion Coefficients					Average Error (pixels)			
$\mathcal{L}$	C_3	C_5	P_1	P_2	$w=0$	$w=1$	$w=2$	$n=5$
#1	10^{-5}	10^{-9}	10^{-5}	10^{-5}	0.002	0.428	0.522	0.391
	10^{-5}	10^{-9}	0.000	0.000	0.004	0.344	0.382	0.246
	10^{-5}	10^{-10}	0.000	0.000	0.281	0.348	0.579	2.818
	10^{-5}	10^{-10}	10^{-6}	10^{-6}	0.007	0.278	0.623	2.782
#2	10^{-5}	10^{-9}	10^{-5}	10^{-5}	0.000	0.151	0.015	0.068
	10^{-5}	10^{-9}	0.000	0.000	0.003	0.305	0.339	0.221
	10^{-5}	10^{-10}	0.000	0.000	0.029	0.152	0.345	1.591
	10^{-5}	10^{-10}	10^{-6}	10^{-6}	0.068	0.192	0.339	1.701
#3	10^{-5}	10^{-9}	10^{-5}	10^{-5}	0.000	0.501	0.574	0.590
	10^{-5}	10^{-9}	0.000	0.000	0.007	0.329	0.330	0.337
	10^{-5}	10^{-10}	0.000	0.000	0.043	0.444	0.488	2.356
	10^{-5}	10^{-10}	10^{-6}	10^{-6}	0.009	0.415	0.645	2.368

Table 3: Results on estimation of Optical center (x_p, y_p)

Distortion Coefficients						Average Error (pixels)		
$\mathcal{L}$	C_3	C_5	P_1	P_2	Grid	$w=0$	$w=1$	$w=2$
#1	10^{-5}	10^{-9}	10^{-5}	10^{-5}	2	0.002	4.232	9.014
	10^{-5}	10^{-9}	10^{-5}	10^{-5}	5	0.002	0.363	10.220
	10^{-5}	10^{-9}	10^{-5}	10^{-5}	10	0.002	0.363	0.390
#2	10^{-5}	10^{-9}	10^{-5}	10^{-5}	2	0.008	4.271	3.792
	10^{-5}	10^{-9}	10^{-5}	10^{-5}	5	0.008	0.663	12.017
	10^{-5}	10^{-9}	10^{-5}	10^{-5}	10	0.008	0.663	0.773

6 Results with Real Images

We used ξ_3 to undistort images captured by both, a $1/2''$ CCD Sony camera with a Computar 3.6mm lens and a $1/3''$ CCD Computar EMH200-L25 Hi-Res board camera with a 2.5mm lens.

The calibration of the images was done using a set of about 10 lines and a total of about 250 points. The estimated distortion parameters obtained using ξ_3 were used to undistort the images (see Figure 5 and Figure 6).

For imaging systems having a large field of view, a perspective projection model may not be appropriate for visualization purposes [Fleck, 1985]. However, the recovery of the distortion parameters facilitates the mapping of the image using any other projection model. For instance, for a wide-angle system, a panoramic projection model or a stereoscopic model may be more suitable.

Using the computed distortion parameters and a projection model, a look-up table can be created that maps im-

(5 a)

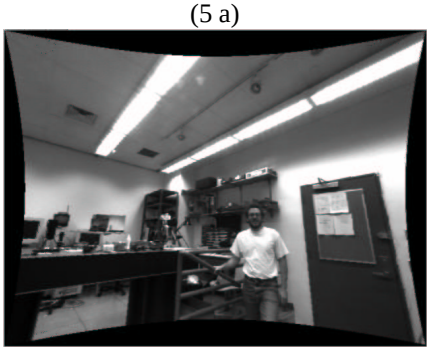

(5 b)

Figure 5: (a) Image captured with a Computar 3.6mm lens and a Sony $1/2''$ CCD camera (b) Distortion parameters recovered via the minimization of ξ_3 are used to map (a) into a perspective image.

(6 a)

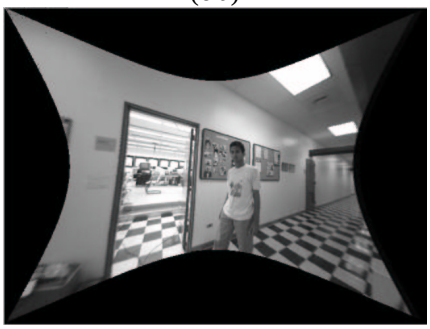

(6 b)

Figure 6: (a) Image captured with a Computar 2.5mm lens and a $1/3''$ CCD board camera. (b) Distortion parameters recovered via the minimization of ξ_3 are used to map (a) into a perspective image.

age points to their new locations. We used such look-up tables to map distorted video streams from wide-angle imaging systems to perspective images in real-time.

References

[Becker and Bove, 1995] S. Becker and V.M. Bove. Semiautomatic 3-d model extraction from uncalibrated 2-d camera views. *In Proc. SPIE Visual Data Exploration and Analysis II*, 2410:447–461, Feb 1995.

[Born and Wolf, 1965] M. Born and E. Wolf. *Principles of Optics*. Permagon Press, 1965.

[Brown, 1966] D.C. Brown. Decentering distortion of lenses. *Photogrammetric Engineering*, 32(3):444–462, May 1966.

[Brown, 1971] D.C. Brown. Close range camera calibration. *Photogrammetric Engineering*, 37(8):855–866, Aug 1971.

[Conrady, 1919] A. Conrady. Decentering lens systems. *Monthly notices of the Royal Astronomical Society*, 79:384–390, 1919.

[Fleck, 1985] M. Fleck. Perspective projection : the wrong imaging model. Technical Report 95-01, University of Iowa, Computer Science, 1985.

[Goshtasby, 1989] A. Goshtasby. Correction of image deformation from lens distortion using bezier patches. *Computer Vision, Graphics, and Image Processing*, 47:385–394, 1989.

[Kang, 1997] S.B. Kang. Semi-automatic methods for recovering radial distortion parameters from a single image. *DEC, Cambridge Research Labs, Technical Reports Series CRL 97/3*, May 1997.

[Nelder and Mead, 1965] J.A. Nelder and R.A. Mead. A simplex method for function minimization. *Computer Journal*, 7:308–313, 1965.

[Stein, 1997] G.P. Stein. Lens distortion calibration using point correspondences. In *Proceedings of the 1997 Conference on Computer Vision and Pattern Recognition*, pages 143–148, San Francisco, June 1997. IEEE Computer Society.

[Tsai, 1987] R.Y. Tsai. A versatile camera calibration technique for high-accuracy 3d machine vision. *International Journal of Robotics and Automation*, 3(4):323–344, Aug 1987.

[Weng *et al.*, 1992] J. Weng, P. Cohen, and M. Herniou. Camera calibration with distortion models and accuracy evaluation. *IEEE Transactions on Pattern Analysis and Machine Intelligence*, 14(10):965–980, Oct 1992.